Science Advances

AAAS

advances.sciencemag.org/cgi/content/full/3/12/e1701211/DC1

Supplementary Materials for

Intracerebroventricular delivery of hematopoietic progenitors results in rapid and robust engraftment of microglia-like cells

Alessia Capotondo, Rita Milazzo, Jose M. Garcia-Manteiga, Eleonora Cavalca, Annita Montepeloso, Brian S. Garrison, Marco Peviani, Derrick J. Rossi, Alessandra Biffi

Published 6 December 2017, *Sci. Adv.* **3**, e1701211 (2017)
DOI: 10.1126/sciadv.1701211

The PDF file includes:

Other Supplementary Material for this manuscript includes the following:
(available at advances.sciencemag.org/cgi/content/full/3/12/e1701211/DC1)

- table S3C (Microsoft Excel format). Genes up-regulated in μCT versus TAμBU_TX as per Fig. 5C.
- table S3D (Microsoft Excel format). Genes down-regulated in μCT versus TAμBU_TX as per Fig. 5D.

Supplementary Materials and Methods

Isolation, transduction and transplantation of murine hematopoietic cells

HSPCs were purified by Lineage$^-$ (Lin$^-$) selection using the Miltenyi Biotec Lineage Cell Depletion Kit with Magnetic separation with the autoMACS™ Separator, following manufacturer's instruction. When KSL (c-kit$^+$ sca-1$^+$) and, among this fraction, CD150$^{+/-}$CD48$^{+/-}$ cell isolation was performed, Lin$^-$ cells were stained with Biotin-Antibody Cocktail (Miltenyi Biotec Lineage Cell Depletion Kit) / Streptavidin Pe-Cy5 (BD Pharmingen) in order to exclude the few Lin$^+$ cells (5-10%) remained after lineage negative selection. For the isolation of the KSL fraction, cells were then stained with rat APC-eFluor 780 anti-mouse CD117(c-kit) (eBioscience) and with rat Pe-cy7 anti-mouse Ly-6A/E Sca-1 (Sca-1) (BD Bioscence). For CD150$^{+/-}$CD48$^{+/-}$ cell selection we added also hamster PE anti-mouse CD48 (Biolegend) and rat APC anti-mouse CD150 (BioLegend). At the end of the staining the cells were isolated by the cell sorter MOFLO XDP (Becton Dickinson), according to the expression of the selected markers. The gated strategy is reporter on Supplementary Fig. 2A. Isolated Lin$^-$, KSL or CD150$^{+/-}$CD48$^{+/-}$ KSL cells were transduced using different Lentiviral Vectors (LVs), for 16 hours at Multiplicity of Infection (MOI) 100. In particular, we used the following LVs: pCCLsin.cPPT.humanPGK.GreenFluorescentProtein.Wpre (GFP-LV) for Lin-, KSL and CD150$^+$CD48$^-$ KSL cells; pCCLsin.cPPT.humanPGK.DeletedNerveGrowthFactorReceptor.Wpre (ΔNGFR-LV) for not-KSL cells and CD150$^-$CD48$^-$ KSL cells; pCCLsin.cPPT.humanPGK.mCherryProtein.Wpre (mCherry-LV) for CD150$^-$ CD48$^+$ KSL cells; pCCLsin.cPPT.humanPGK.Tag-BlueFluorescentProtein.Wpre (Tag-BFP-LV) for CD150$^+$CD48$^+$ KSL cells. A fraction of the transduced cells were cultured for 10 days in vitro in order to assess transgene expression by cytofluorimetric analysis. Transduced cells were injected via the tail vein or ICV into seven/eight-week-old conditioned C57BL6/J female mice, 24 hours after irradiation (2x400cGy) or the fourth busulfan dose (25mg/kg x four days), at different concentration according to the different experimental settings:

IV transplantation

Lin$^-$cells: 10^6 cells/mouse; KSL: $0.3x10^5$ cells/mouse; Not KSL: $5x10^5$ cells/mouse; HPC1≅$0,12x10^4$ cells/mouse; LT-HSC≅$0,55x10^4$ cells/mouse; HPC2≅$1,8x10^4$ cells/mouse; MPPs≅$0,55x10^4$ cells/mouse. Five days after transplantation of KSL cells, mice received $5x10^5$ of total bone marrow (TBM) cells from CD45.1 C57 mice as support. Mice were maintained in sterile conditions.

ICV transplantation

Lin$^-$cells: $0.3x10^6$ cells/mouse; KSL: $0.3x10^5$ cells/mouse; Not KSL: $3x10^5$ cells/mouse; HPC1≅$0,12x10^4$ cells/mouse; LT-HSC≅$0,55x10^4$ cells/mouse; HPC2≅$1,8x10^4$ cells/mouse; MPPs≅$0,55x10^4$ cells/mouse. Five days after transplantation, mice received $5x10^5$ of TBM cells from CD45.1 C57 mice as support.

For isolation of Fgd5 HSCs, 8 weeks Fgd5$^{ZsGr\cdot ZsGr/+}$ CD45.2 mice (The Jackson Laboratory Stock # 027788) were used as donors. Enrichment of c-kit+ cells was performed using CD117 (c-kit) MicroBeads (CD117 MicroBeads, mouse – Miltenyi Biotec) following manufacturer's instruction. c-kit enriched cells were then stained in PBS 2 mM EDTA, 2% FBS at 4°C with combinations of the following antibodies: the lineage markers Ter119, Mac-1 (m1/70), Gr-1 (8C5), CD3 (17A2), CD4 (RM4-5), CD8 (53–6.7), B220 (RA3-6B2), and IL7Ra (A7R34); CD34 (RAM34), Flk2(A2F10), c-kit (2B8), Sca1 (D7), CD45.2 (104) (all from BioLegend or eBioscience). After staining, cells were washed and resuspended in PBS 2 mM EDTA, 2% FBS with PI (0.05 µg/ µL), and kept on ice. FACSAria II (BD) was used for cell sorting.

Sorted cells were transplanted IV (500) or ICV (500). Five days after transplantation, mice received 1.0*10^6 TBM from CD45.1 C57 mice as support.

Recipients of cell transplantation were 2-month old female CD45.2 C57BL6/J mice conditioned with 25-27mg/kg of busulfan (Sigma) administered i.p. or with a lethal irradiation dose (2x500cGy). For IV transplantation cells were injected in the tail vein. ICV transplantation was performed by surgery, upon

anesthesia (ketamine (100mg/kg) and xylazine (10mg/kg). The head of the mouse, shaved and disinfected, was fixed with ear bars in a stereotactic frame and the skin was disclosed longitudinally. Bregma was visualized and coordinates were recorded. From bregma, injection coordinates (1 mm lateral, - 0.5 mm anterior) were adjusted before the cranial bone was enclosed under visual control with a drill head of 0.7mm diameter. Five µl of the cell suspension were injected through a 10µl Hamilton syringe upon insertion into the brain 2mm distal from the cranial bone. Following wound closure, animals received a single dose of atipamezole (1µl/g) and were maintained in sterile conditions.

Prophylactic Antibiotic (Gentamycin Sulfate, 80mg/250mL) was administered via the drinking water for 2 weeks following conditioning and transplantation. Depending on the strain and experimental setting, mice were sacrificed 1.5, 3, 4 and 6 months spo-transplant, and peripheral blood/BM and brain were analyzed for donor cell engraftment.

Isolation, transduction and transplantation of human CD34$^+$ cells

Human cord blood (CB)-derived CD34$^+$ cells were purchased from Lonza (2C-101). Upon thawing, cells were pre-stimulated for 24 hours in CellGro medium (CellGenix, Freiburg, Germany) supplemented with hIL-3 [60 ng/µL], hTPO [100 ng/µL], hSCF [300 ng/µL], hFlt3-L [300 ng/µL] (all of them from Peprotech, Hamburg, Germany) and transduced by one round of LV exposure at MOI 100 with GFP- or ARSA encoding laboratory grade LVs. A fraction of the transduced cells was cultured for 10 days in vitro in order to assess transgene expression. After transduction, the cells were washed and infused into the tail vein of sublethally irradiated (200cGy) or busulfan-treated (16.25 mg/kg/day for four days) 7 to 9-week-old female NSG mice. We transplanted 5x10^5 hCD34$^+$ cells/mouse both IV and ICV. ICV transplantation of hCD34$^+$ cells in NSG mice was performed as described for murine HSPC ICV transplantation in C57 mice. When NSG mice were pre-treated with busulfan, we transplanted 4x10^6 TBM from male NSG mice as support. After 12 weeks

mice were sacrificed and BM and brain were analyzed for human hematopoietic cell engraftment.

Post-natal day 2 *Rag*$^{-/-}$*γ-chain*$^{-/-}$As2$^{-/-}$ were conditioned with a sub-lethal dose of 300+250 RAD total body irradiation. Mice received transduced cells IV via temporal vein injection (2.5x10^{5}cells/mouse) or ICV (in the lateral ventricle through a glass capillary) (0.75x10^{5}cells/mouse). Five weeks post-transplant mice were sacrificed and BM and brain were analyzed for human hematopoietic cell engraftment by cytofluorimetry and ARSA activity by using 4-methylumbelliferyl-sulfate substrate.

Mouse tissue collection and processing for flow cytometry and histology

Mice were euthanized under deep anesthesia by extensive intra-cardiac perfusion with cold PBS for 15 minutes after clumping the femur. Organs were then collected and differentially processed. Bone marrow (BM) cells were collected from the clumped femur as described. Brain was removed and the two hemispheres were differently processed. For immunofluorescence analysis, one hemisphere was fixed for 24 hours in 4% PFA, embedded in OCT compound and stored at -80°C, after equilibration in sucrose gradients (from 10 to 30%). For flow cytometry analysis, cells from the other hemisphere were mechanically disaggregated to obtain a single cell suspension in 20ml of GKN/BSA buffer (8g/L NaCl, 0.4 g/L KCl, 1.42 g/L NaH2P04, 0.93 g/L Na2HP04, 2 g/L D+ Glucose, pH 7.4 + 0.002% BSA). For the analysis of Fgd5$^+$ cell engraftment, hCD34$^+$ derived cell engraftment in the brain of NSG and *Rag*$^{-/-}$*γ–chain*$^{-/-}$As2$^{-/-}$ transplanted mice, we performed an enrichment for myeloid cells using a 30% Percoll gradient after enzymatic (19 mg papain, 10 mg cystein, 2,5 mg DNAse) digestion of the brain tissue.

Flow-cytometric analysis

Cells from BM and brain were analyzed by flow cytometry upon re-suspension in blocking solution (PBS 5%FBS, 1%BSA) and labeling at 4°C for 15 minutes

with the following specific antibodies: rat PE anti-mouse CD45 (BD Pharmingen) 1:100; rat APC anti-mouse CD45 (BD Biosciences) 1:150; rat Brilliant Violet 510 anti-mouse CD45, (BioLegend) 1:150; rat Pacific Blue anti-mouse CD45.2 (Bio Legend) 1:100; mouse PE anti-Mouse CD45.1 (BD bioscience) 1:100; rat APC anti-mouse CD11b (eBioscience) 1:100; mouse Alexa Fluor 647 anti-Human CD271 (NGF receptor) (BD Pharmingen) 1:30; rat APC 780 anti-mouse CD11b (eBioscience) 1:100; rat APC 780 anti-mouse CD117(c-kit) (eBioscience) 1:100; rat PE-Cy7 anti- mouse Ly-6A/E Sca-1 (Sca-1) (BD Bioscence) 1:150; Hamster PE anti-mouse CD48 (Biolegend) 1:100; rat APC anti-mouse CD150 (Biolegend) 1:75; rat PE anti-mouse CD202b (Tie2) (eBioscence) 1:150; rat PE anti-mouse CD184 (CXCR4) (BD Bioscence) 1:150; rat PE anti-mouse CD34 (eBioscience) 1:150; rat PE-Cy7 anti-mouse CD93 (AA4.1) (eBioscience) 1:150; rat Biotin anti-mouse CD115 (eBioscience) 1:150; goat APC anti-mouse CX3CR1 (R&D systems) 1:75; APC streptavidin (BD Pharmingen) 1:500; rat APC-Cy7 anti-mouse B220 (BD Bioscience) 1:100; hamster APC-Cy7 anti-mouse CD3e (eBiosciences) 1:100; mouse APC-Cy7 anti-human CD45 (BD Pharmingen); rat PE-cy7 anti-human CX3CR1 (eBioscience) 5:100. For the exclusion of death cells we either used 7-AAD (1mg/ml) (Sigma-Aldrich), a membrane-impermeable dye, added to the cells prior to analysis for dead cell exclusion.

BM and brain cells were analyzed by LSR Fortessa (Beckton Dickinson).

Immunofluoresce analysis

Brains were serially cut in the sagittal planes on a cryostat in 15µm sections. Tissue slides were washed twice with PBS, air dried and blocked with 0.3% Triton, 2% BSA, 10% NGS (Vector Laboratories) for 2 hours. Then sections were incubated over night with primary antibodies diluted in PBS, 0.1% Triton, 2% BSA, 10% NGS at 4°C as follows: rat APC anti CD11b (eBioscience) 1:50; rabbit anti Iba1 (Wako) 1:100; chicken anti-GFP (Abcam) 1:250; rabbit anti GFP (Invitrogen) 1:100; mouse PE anti-human CD271 (NGF Receptor) (BD Pharmingen) 1:50; rabbit anti-cherry (Abcam) 1:100. The secondary antibodies goat IgG anti-Chicken Alexa Fluor 488, goat IgG anti-Rabbit Alexa Fluor 488, 546 or 633, goat IgG anti-Rat Alexa Fluor 546 or 633, goat IgG

anti-Mouse Alexa Fluor 546 (Molecular Probes, Invitrogen) were diluted 1:500 in the same blocking solution used for primary antibodies staining and incubated with sections for 2 hours at room temperature. Nuclei were stained with Topro III (Molecular Probes, Invitrogen) 1:1000 in PBS or by DAPI (Roche) 1:30 in PBS. Slices were washed in PBS, air dried and mounted with Fluorsafe Reagent (Calbiochem). Not transplanted mice were used as negative controls for the reporter transgene staining. Incubation with secondary antibody alone was performed in order to exclude the background signal. Samples were analyzed with a confocal microscope (Zeiss and Leica TCS SP2; Leica Microsystems Radiance 2100; Bio-Rad) (λexcitation = 488, 586, 660). Fluorescent signal was processed by Lasersharp 2000 software. Images were imported into Adobe Photoshop CS 8.0 software and processed by using automated level correction. For the reconstruction of brain sections we used a fluorescence microscope Delta Vision Olympus Ix70 for the acquisition of the images, which were then processed by the Soft Work 3.5.0 software. Images were then imported into the Adobe Photoshop CS 8.0 software and reconstructed.

RNA extraction and gene expression analysis by real time PCR

Total RNA was isolated for gene expression analysis from the following populations previously sorted from adult or P10 naïve control and transplanted mice: total $CD45^+CD11b^+$, μ and TAμ, sorted according to the expression of CD45, CD11b and GFP (only HCT-mice); macrophages, sorted from bone marrow according to the expression of CD45, CD11b, F4/80, Ly6C and GFP (only HCT-mice). RNA quantity was determined using QuantiFluor® RNA system and Quantus™ Fluorometer (Promega). cDNA was generated starting from 1 ng up to 100ng of purified mRNA by using SuperScript VILO Master mix (Thermo Fisher Scientific). cDNA was then pre-amplified using Custom Taqman® PreAmp Pools (Thermo Fisher Scientific). Thermal cycling for cDNA generation and preamplification was performed on T100 Thermal cycler (BIO-RAD) following manufacturer's instructions. Gene expression analysis was performed using a custom design TaqMan-based microfluidic card gene expression assay (Applied Biosystems) to measure the expression of 16 selected genes (13 targets, 2 endogenous housekeeping and 1 internal

control). Real time PCR was run in standard mode on Applied Biosystems® ViiA™ 7 Real-Time PCR System, using the following thermal cycling conditions: one cycle at 50°C for 2 min, one cycle at 95°C for 10 min, 40 cycles at 95°C for 15 seconds and 60°C for 1 min. (Applied Biosystems). The ViiA™ 7 Software v1.2.2 was used to extract raw data. The difference (dCT) between the threshold cycle (CT) of each gene and that of the reference gene (mean of HPRT and 18S CTs) was used to determine gene expression. Fold change expression of selected microglia genes in ICV versus IV transplanted mice was calculated by 2^{-ddCT} method, where ddCT represents the difference between the dCT of each samples retrieved from ICV transplanted mice and the dCT mean of the samples retrieved from IV transplanted mice, matched for μ and TAμ cells.

RNA sequencing and analysis

RNeasy Plus Micro kit (Qiagen) was used to extract RNA from the sorted myeloid brain populations. In particular, we retrieved by sorting different myeloid brain sub-populations from: P10 (n=4 in duplicate) (TAμ cells), 5 month old C57bl6/j (n=3) mice (μ cells), and BU-treated mice (n=3; we excluded from the analysis one sample of TAμ due to its diversity from the other samples analyzed by FACS)(μ and TAμ cells) at 3 months from GFP HSPC transplantation. Before the sorting, mice were euthanized under deep anesthesia by intra-cardiac perfusion with cold PBS after clumping the femur. The brain was collected and processed as described before. RNA was collected and stored at - 80°C. Small aliquot were used to check the quality of the RNA extracted with Agilent RNA 6000 Pico kit. Samples with RIN below 7 were excluded from the analysis.

RNA sequencing was performed by IGA Technology Services at Udine. Briefly, amplification of cDNA from total RNA (starting amount =100 ng per sample) was performed using the Ovation RNA-Seq System V2 (Nugen), cDNA was then fragmented and ligated into a sequencing library using NuGEN's Ovation Ultralow Library Systems. After barcoding, the RNA libraries were pooled, denatured and diluted to an 8 pM final concentration. Cluster formation was performed on cBot (Illumina) (single-end) using flow

cells v.3. The SBS (sequencing by synthesis) was performed according to TruSeq SR protocol (Illumina) for the HiSeq 2500 (Illumina) set to 50 cycles, yielding an average of $30x10^6$ clusters for each sample. Raw sequences (fastq) were filtered for good quality scores using FastQC software. Sequences obtained were aligned to the Mouse genome (mm10 release) using STAR aligner (STAR_2.3.0e_r291). Only uniquely mapped reads were used to estimate gene counts using the reported Ensembl gene annotations (v72) through the Python script 'HTSeq-count' (model type – union, http://www-huber.embl.de/users/anders/HTSeq/). Subsequent to mapping the gene count data was normalized using the "weighted trimmed mean of M-values". After normalization, differential gene expression was performed using the "limma" package in R.

Statistical analysis on RNA sequencing

Principal Component Analysis (PCA)

PCA was made using ***mixOmics*** library in R (2. mixOmics: Omics Data Integration Project. R package version 6.0.0. https://CRAN.R-project.org/package=mixOmics) on $\log_2$ normalized expression values generated by the *voom* function in ***limma***.

Hierarchical Clustering

Hierarchical clustering was made using the ***pheatmap*** function of the R library with the same name ('Euclidean distance' and 'complete' method.) on $\log_2$ normalized expression values generated by the *voom* function in ***limma***.

Analysis of RNA-Seq data

We downloaded raw expression data from control microglia and macrophages of diverse origin in the GEO dataset GSE62826 from SRA archive (SRR1634675, SRR1634676, SRR1634677, SRR1634678, SRR1634708, SRR1634709, SRR1634710, SRR1634711, SRR1634712, SRR1634721) and fastq files with raw sequences were obtained. Reads from from Gosselin macrophages and microglia were processed together with reads from our μ and TAμ cells (see above) and PCA and heatmaps were produced in order to compare our μ and TAμ populations' expression

with both adult microglia and macrophages in the study of Gosselin et al..

Functional Enrichment

To evaluate pathways related to differences between cell populations, GSEA pre-ranked analysis was performed. Lists of log2FoldChanges estimated with limma were used as pre-ranked lists with gsea pre-reanked command line tool with default parameters (gsea2-2.2.3.jar). Gene Ontology Biological Processes (c5.go.bp) was used as gmt file after translating human entrez id to mouse gene symbols using ensembl-mart homology maps. Due to the higher number of significant categories found correlated to µ.BUTX and TAµ.BUTX cells, the standard FDR cut off for the enrichment was increased from 0.05 to 0.001. GOSemSim semantic similarities matrix was calculated using GOSemSim R package. The matrix of similarities was shown as heatmap of clustered GOs using *pheatmap* in R (with “euclidean” distance and “complete” method for clustering).

Accession codes.

Gene Expression Omnibus: RNA-Seq data are available under accession code GSE87799 and data re-analyzed from Gosselin et al. was available under the accession code GSE62826.

SUPPLEMENTARY FIGURES

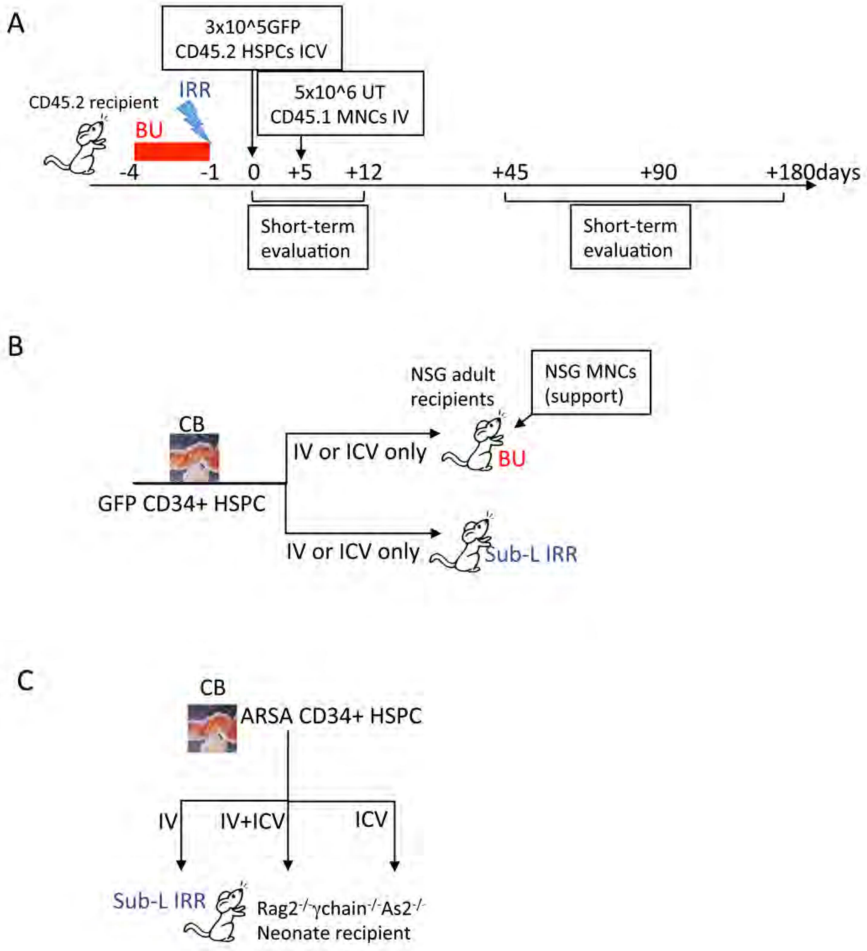

fig. S1. Experimental schemes for the different transplantation settings described in the paper, using both mouse and human HSPCs. (**A**) Experimental scheme of Lin$^-$ HSPC ICV transplantation in myeloablated mice (BU: myeloablation by busulfan treatement; IRR: lethally irradiation). Different time points of analysis are indicated. (**B**) Experimental scheme showing the transplant protocol for human CB CD34+ cells transplanted either IV or ICV into busulfan- myeloablated (BU) or sub-lethally irradiated (Sub-L-IRR) NSG adult mice (See SI Material and Methods for details) after LV transduction. (**C**) Experimental scheme for human CB CD34$^+$ cells transplantation by either IV, IV + ICV or ICV only routes into sub-lethally irradiated (Sub-L-IRR) Rag2$^{-/-}$γ-chain$^{-/-}$As2$^{-/-}$ neonate mice. Mononuclear cells (MNC), untransduced (UT).

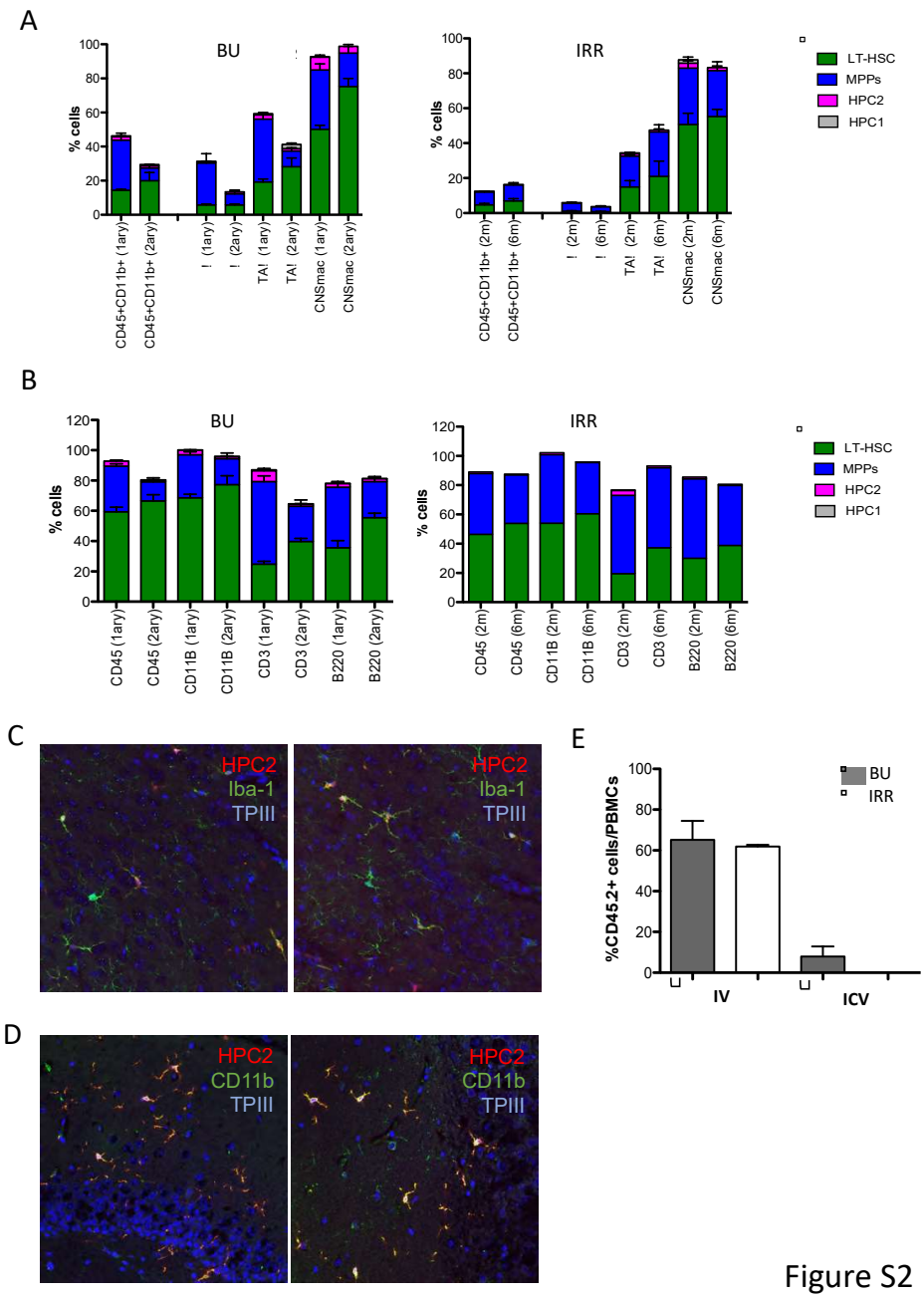

Figure S2

fig. S2. Analysis of the engraftment of murine HSPC subpopulations in BU_TX or irradiated mice. (**A** and **B**) Frequency of cells derived from each of the transplanted KSL sub-populations within total brain myeloid cells, µ and TAµ cells (A), and total CD45+ hematopoietic bone marrow (BM) cells, myeloid (CD11b) and lymphoid (CD3 and B220) lineages (B) of busulfan-treated transplanted (BU_TX) (left), and irradiated transplanted (IRR)(right) mice at different time points post-HCT. BU_TX primary (1ary) recipients were used as donors for 2ary recipients (see text for details). N=10 mice/group. (**C**)

Immunofluorescence analysis for IBA-1+ (C) and CD11b+ (**D**) (both in green) and HPC2 (red, Cherry+) cells on brain sections from BU_TX mice at 60 days after ICV transplantation. M= merge. Topro III (TPIII) (blu) for detection of nuclei. M=merge. Magnification 20x. Images were acquired at confocal microscope Radiance 2100 (Bio-Rad) Ix70 and processed by the Soft Work 3.5.0. (**E**) Frequency of donor cells (CD45.2+) within PBMCs of BU-TX and IRR mice transplanted with FGD5+ cells IV and ICV, at sacrifice 4 months post-transplantation. N≥4 per group.

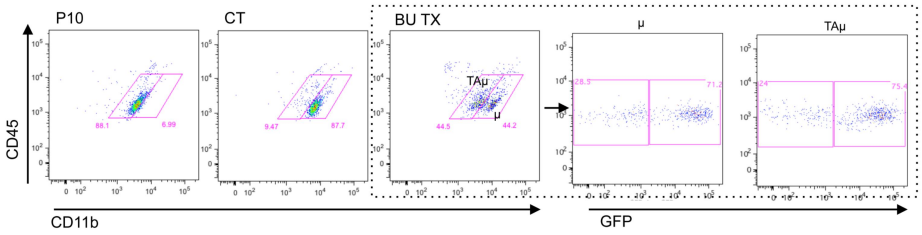

fig. S3. FACS plots of cell populations sorted for gene expression analysis. Representative dot plots showing the cell populations sorted for gene expression analysis. In particular μ and TAμ, identified by the CD45 and CD11b markers, in the brain of naïve P10 and adult control (ADULT_CT) animals, and busulfan-treated and transplanted mice (BU_TX) at 90 days after HCT are shown. The dot plots included in the dotted square show both GFP^- endogenous cells and GFP^+ donor derived cell chimerism within μ and TAμ populations of a representative transplanted BU-treated mouse.

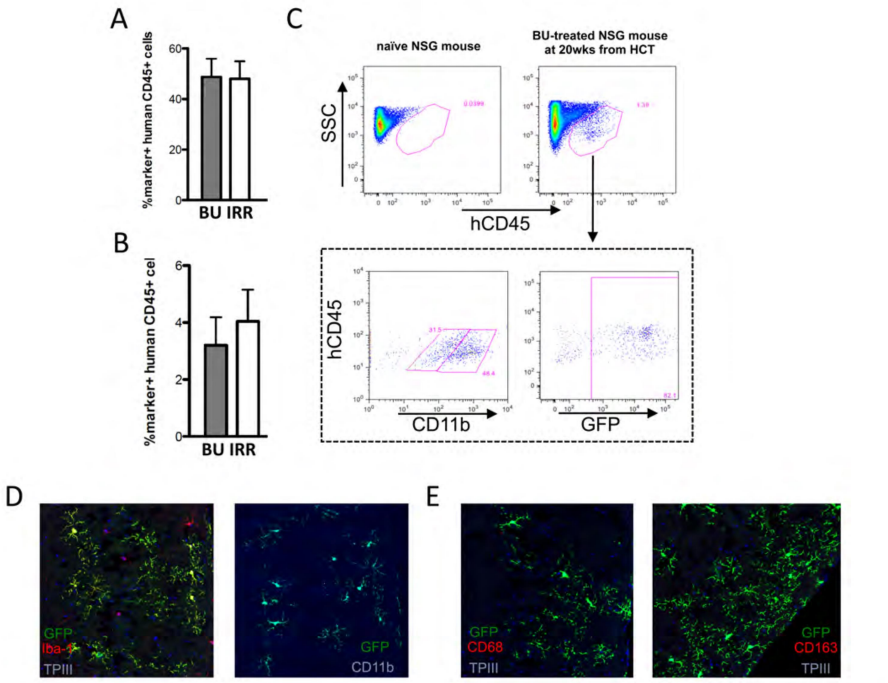

fig. S4. Evaluation of hCD34$^+$ cell engraftment in BM and brain of transplanted NSG mice. (**A** and **B**) Frequency of human CD45$^+$ cells retrieved in BM (A) and brain (B) of NSG mice transplanted with GFP LV transduced CB CD34$^+$ cells after sub-lethal irradiation (IRR) or BU-treatment (BU), 12 weeks from IV transplantation. N≥5 mice/group. (**C**) Representative dot plot showing the gating strategy for the identification of human CD45$^+$ CD11b$^+$ and GFP$^+$ cells in the brain of NSG mice. (**D** and **E**) Immunofluorescence analysis of brain slices from BU_TX NSG mice transplanted with human CD34$^+$ cells at 12 weeks from the transplant showing GFP$^+$ (green), Iba$^+$ (red) (in D) and CD68$^-$ (red) (on the left) or CD163$^-$ (red) cells (on the right)(E). Topro III (TPIII) (blu) for detection of nuclei. M=merge. Magnification 40x. Images were acquired at confocal microscope Radiance 2100 (Bio-Rad) Ix70 and processed by the Soft Work 3.5.0.

table S1. ANOVA *P* values with Tukey's post hoc test of contrasts between cells in Fig. 4B.

* p < 0.05; ** p < 0.01; *** p< 0.001

Tmem	P.value.Tukey's	Signficance Level
ICV TAmu GFP+-AD Mac CO	0,08	NS
ICV mu GFP+-AD Mac CO	0,00	**
IV TAmu GFP+-AD Mac CO	0,97	NS
IV TAmu GFP--AD Mac CO	0,84	NS
IV TAmu TOT-AD Mac CO	0,09	NS
IV muGFP+-AD Mac CO	0,43	NS
IV muGFP--AD Mac CO	0,00	**
IV muTOT-AD Mac CO	0,00	**
TAmu p10-AD Mac CO	0,99	NS
ICV mu GFP+-ICV TAmu GFP+	0,73	NS
IV TAmu GFP+-ICV TAmu GFP+	0,50	NS
IV TAmu GFP--ICV TAmu GFP+	0,77	NS
IV TAmu TOT-ICV TAmu GFP+	1,00	NS
IV muGFP+-ICV TAmu GFP+	0,99	NS
IV muGFP--ICV TAmu GFP+	0,58	NS
IV muTOT-ICV TAmu GFP+	0,62	NS
TAmu p10-ICV TAmu GFP+	0,43	NS
IV TAmu GFP+-ICV mu GFP+	0,02	*
IV TAmu GFP--ICV mu GFP+	0,04	*
IV TAmu TOT-ICV mu GFP+	0,68	NS
IV muGFP+-ICV mu GFP+	0,18	NS
IV muGFP--ICV mu GFP+	1,00	NS
IV muTOT-ICV mu GFP+	1,00	NS
TAmu p10-ICV mu GFP+	0,01	*
IV TAmu GFP--IV TAmu GFP+	1,00	NS
IV TAmu TOT-IV TAmu GFP+	0,56	NS
IV muGFP+-IV TAmu GFP+	0,97	NS
IV muGFP--IV TAmu GFP+	0,01	*
IV muTOT-IV TAmu GFP+	0,02	*
TAmu p10-IV TAmu GFP+	1,00	NS
IV TAmu TOT-IV TAmu GFP-	0,81	NS
IV muGFP+-IV TAmu GFP-	1,00	NS
IV muGFP--IV TAmu GFP-	0,03	*
IV muTOT-IV TAmu GFP-	0,05	NS
TAmu p10-IV TAmu GFP-	1,00	NS
IV muGFP+-IV TAmu TOT	0,99	NS
IV muGFP--IV TAmu TOT	0,52	NS

IV muTOT-IV TAmu TOT	0,57	NS
TAmu p10-IV TAmu TOT	0,49	NS
IV muGFP--IV muGFP+	0,13	NS
IV muTOT-IV muGFP+	0,18	NS
TAmu p10-IV muGFP+	0,95	NS
IV muTOT-IV muGFP-	1,00	NS
TAmu p10-IV muGFP-	0,01	**
TAmu p10-IV muTOT	0,02	*
Tgbr1	**p adj**	
ICV TAmu GFP+-AD Mac CO	0,047770938	*
ICV mu GFP+-AD Mac CO	0,002134432	**
IV TAmu GFP+-AD Mac CO	0,991484632	NS
IV TAmu GFP--AD Mac CO	0,998580306	NS
IV TAmu TOT-AD Mac CO	0,561025873	NS
IV muGFP+-AD Mac CO	0,951171064	NS
IV muGFP--AD Mac CO	0,715322778	NS
IV muTOT-AD Mac CO	0,154136228	NS
TAmu p10-AD Mac CO	0,999965681	NS
ICV mu GFP+-ICV TAmu GFP+	0,831298021	NS
IV TAmu GFP+-ICV TAmu GFP+	0,517641085	NS
IV TAmu GFP--ICV TAmu GFP+	0,210609456	NS
IV TAmu TOT-ICV TAmu GFP+	0,924426753	NS
IV muGFP+-ICV TAmu GFP+	0,466632934	NS
IV muGFP--ICV TAmu GFP+	0,955342056	NS
IV muTOT-ICV TAmu GFP+	1	NS
TAmu p10-ICV TAmu GFP+	0,125905113	NS
IV TAmu GFP+-ICV mu GFP+	0,061199767	NS
IV TAmu GFP--ICV mu GFP+	0,011726154	*
IV TAmu TOT-ICV mu GFP+	0,189000424	NS
IV muGFP+-ICV mu GFP+	0,036279599	*
IV muGFP--ICV mu GFP+	0,30390729	NS
IV muTOT-ICV mu GFP+	0,929590463	NS
TAmu p10-ICV mu GFP+	0,006268098	**
IV TAmu GFP--IV TAmu GFP+	0,999999541	NS
IV TAmu TOT-IV TAmu GFP+	0,994550436	NS
IV muGFP+-IV TAmu GFP+	0,999999996	NS
IV muGFP--IV TAmu GFP+	0,997956308	NS
IV muTOT-IV TAmu GFP+	0,709890916	NS
TAmu p10-IV TAmu GFP+	0,999905255	NS
IV TAmu TOT-IV TAmu GFP-	0,934399448	NS
IV muGFP+-IV TAmu GFP-	0,999936873	NS
IV muGFP--IV TAmu GFP-	0,971780266	NS

IV muTOT-IV TAmu GFP-	0,434774367	NS
TAmu p10-IV TAmu GFP-	0,999999672	NS
IV muGFP+-IV TAmu TOT	0,997281275	NS
IV muGFP--IV TAmu TOT	1	NS
IV muTOT-IV TAmu TOT	0,97798928	NS
TAmu p10-IV TAmu TOT	0,830556294	NS
IV muGFP--IV muGFP+	0,999222858	NS
IV muTOT-IV muGFP+	0,706102184	NS
TAmu p10-IV muGFP+	0,997979213	NS
IV muTOT-IV muGFP-	0,984900869	NS
TAmu p10-IV muGFP-	0,913443177	NS
TAmu p10-IV muTOT	0,308018851	NS
P2ry13	**p adj**	
ICV TAmu GFP+-AD Mac CO	0,985301461	NS
ICV mu GFP+-AD Mac CO	0,939016036	NS
IV TAmu GFP+-AD Mac CO	0,99997385	NS
IV TAmu GFP--AD Mac CO	0,890618017	NS
IV TAmu TOT-AD Mac CO	0,995194518	NS
IV muGFP+-AD Mac CO	0,326553591	NS
IV muGFP--AD Mac CO	0,007927757	**
IV muTOT-AD Mac CO	0,799633655	NS
TAmu p10-AD Mac CO	0,929964695	NS
ICV mu GFP+-ICV TAmu GFP+	0,99999948	NS
IV TAmu GFP+-ICV TAmu GFP+	0,999984364	NS
IV TAmu GFP--ICV TAmu GFP+	0,999922109	NS
IV TAmu TOT-ICV TAmu GFP+	1	NS
IV muGFP+-ICV TAmu GFP+	0,820488079	NS
IV muGFP--ICV TAmu GFP+	0,038143092	*
IV muTOT-ICV TAmu GFP+	0,996759716	NS
TAmu p10-ICV TAmu GFP+	0,999992619	NS
IV TAmu GFP+-ICV mu GFP+	0,999412113	NS
IV TAmu GFP--ICV mu GFP+	0,999999854	NS
IV TAmu TOT-ICV mu GFP+	0,999996457	NS
IV muGFP+-ICV mu GFP+	0,927037779	NS
IV muGFP--ICV mu GFP+	0,066028225	NS
IV muTOT-ICV mu GFP+	0,999760171	NS
TAmu p10-ICV mu GFP+	1	NS
IV TAmu GFP--IV TAmu GFP+	0,996474386	NS
IV TAmu TOT-IV TAmu GFP+	0,999998401	NS
IV muGFP+-IV TAmu GFP+	0,743792394	NS
IV muGFP--IV TAmu GFP+	0,056042702	NS
IV muTOT-IV TAmu GFP+	0,978653692	NS

TAmu p10-IV TAmu GFP+	0,998713038	NS
IV TAmu TOT-IV TAmu GFP-	0,999825642	NS
IV muGFP+-IV TAmu GFP-	0,986252671	NS
IV muGFP--IV TAmu GFP-	0,15648549	NS
IV muTOT-IV TAmu GFP-	0,999996955	NS
TAmu p10-IV TAmu GFP-	1	NS
IV muGFP+-IV TAmu TOT	0,828879177	NS
IV muGFP--IV TAmu TOT	0,051779067	NS
IV muTOT-IV TAmu TOT	0,995621806	NS
TAmu p10-IV TAmu TOT	0,999974512	NS
IV muGFP--IV muGFP+	0,660689489	NS
IV muTOT-IV muGFP+	0,999857448	NS
TAmu p10-IV muGFP+	0,972120335	NS
IV muTOT-IV muGFP-	0,442837244	NS
TAmu p10-IV muGFP-	0,126116629	NS
TAmu p10-IV muTOT	0,999971633	NS
Mertk	**p adj**	
ICV TAmu GFP+-AD Mac CO	0,646846338	NS
ICV mu GFP+-AD Mac CO	0,013551025	*
IV TAmu GFP+-AD Mac CO	0,996482506	NS
IV TAmu GFP--AD Mac CO	0,999422951	NS
IV TAmu TOT-AD Mac CO	0,702391208	NS
IV muGFP+-AD Mac CO	0,970829778	NS
IV muGFP--AD Mac CO	0,640395697	NS
IV muTOT-AD Mac CO	0,706788687	NS
TAmu p10-AD Mac CO	0,999899073	NS
ICV mu GFP+-ICV TAmu GFP+	0,372808349	NS
IV TAmu GFP+-ICV TAmu GFP+	0,997468573	NS
IV TAmu GFP--ICV TAmu GFP+	0,960128035	NS
IV TAmu TOT-ICV TAmu GFP+	1	NS
IV muGFP+-ICV TAmu GFP+	0,999209731	NS
IV muGFP--ICV TAmu GFP+	0,999999999	NS
IV muTOT-ICV TAmu GFP+	0,999999943	NS
TAmu p10-ICV TAmu GFP+	0,926258801	NS
IV TAmu GFP+-ICV mu GFP+	0,209904368	NS
IV TAmu GFP--ICV mu GFP+	0,060547719	NS
IV TAmu TOT-ICV mu GFP+	0,492186982	NS
IV muGFP+-ICV mu GFP+	0,162559838	NS
IV muGFP--ICV mu GFP+	0,558810484	NS
IV muTOT-ICV mu GFP+	0,764373284	NS
TAmu p10-ICV mu GFP+	0,045753579	*
IV TAmu GFP--IV TAmu GFP+	0,999999872	NS

IV TAmu TOT-IV TAmu GFP+	0,997751476	NS
IV muGFP+-IV TAmu GFP+	0,99999999	NS
IV muGFP--IV TAmu GFP+	0,99497361	NS
IV muTOT-IV TAmu GFP+	0,994608217	NS
TAmu p10-IV TAmu GFP+	0,999996367	NS
IV TAmu TOT-IV TAmu GFP-	0,968484691	NS
IV muGFP+-IV TAmu GFP-	0,999957227	NS
IV muGFP--IV TAmu GFP-	0,947907538	NS
IV muTOT-IV TAmu GFP-	0,956733839	NS
TAmu p10-IV TAmu GFP-	1	NS
IV muGFP+-IV TAmu TOT	0,999316055	NS
IV muGFP--IV TAmu TOT	1	NS
IV muTOT-IV TAmu TOT	0,99999999	NS
TAmu p10-IV TAmu TOT	0,941450225	NS
IV muGFP--IV muGFP+	0,99797833	NS
IV muTOT-IV muGFP+	0,99774539	NS
TAmu p10-IV muGFP+	0,999700818	NS
IV muTOT-IV muGFP-	1	NS
TAmu p10-IV muGFP-	0,911244016	NS
TAmu p10-IV muTOT	0,927947339	NS
Ofml3	**p adj**	
ICV TAmu GFP+-AD Mac CO	0,264083484	NS
ICV mu GFP+-AD Mac CO	0,016898942	*
IV TAmu GFP+-AD Mac CO	0,963909854	NS
IV TAmu GFP--AD Mac CO	0,946977812	NS
IV TAmu TOT-AD Mac CO	0,671076776	NS
IV muGFP+-AD Mac CO	0,566264956	NS
IV muGFP--AD Mac CO	0,002650778	**
IV muTOT-AD Mac CO	0,315318391	NS
TAmu p10-AD Mac CO	0,564339201	NS
ICV mu GFP+-ICV TAmu GFP+	0,765144434	NS
IV TAmu GFP+-ICV TAmu GFP+	0,982466017	NS
IV TAmu GFP--ICV TAmu GFP+	0,947807191	NS
IV TAmu TOT-ICV TAmu GFP+	0,999709077	NS
IV muGFP+-ICV TAmu GFP+	0,999985265	NS
IV muGFP--ICV TAmu GFP+	0,253354688	NS
IV muTOT-ICV TAmu GFP+	0,999998381	NS
TAmu p10-ICV TAmu GFP+	0,99998623	NS
IV TAmu GFP+-ICV mu GFP+	0,345367583	NS
IV TAmu GFP--ICV mu GFP+	0,199843756	NS
IV TAmu TOT-ICV mu GFP+	0,491180435	NS
IV muGFP+-ICV mu GFP+	0,595206514	NS

IV muGFP--ICV mu GFP+	0,995563914	NS
IV muTOT-ICV mu GFP+	0,97405668	NS
TAmu p10-ICV mu GFP+	0,597138664	NS
IV TAmu GFP--IV TAmu GFP+	1	NS
IV TAmu TOT-IV TAmu GFP+	0,999946856	NS
IV muGFP+-IV TAmu GFP+	0,999516968	NS
IV muGFP--IV TAmu GFP+	0,092438986	NS
IV muTOT-IV TAmu GFP+	0,96118073	NS
TAmu p10-IV TAmu GFP+	0,999500054	NS
IV TAmu TOT-IV TAmu GFP-	0,999690708	NS
IV muGFP+-IV TAmu GFP-	0,9978807	NS
IV muGFP--IV TAmu GFP-	0,038794759	*
IV muTOT-IV TAmu GFP-	0,918596797	NS
TAmu p10-IV TAmu GFP-	0,997816021	NS
IV muGFP+-IV TAmu TOT	0,999999995	NS
IV muGFP--IV TAmu TOT	0,127784098	NS
IV muTOT-IV TAmu TOT	0,997015669	NS
TAmu p10-IV TAmu TOT	0,999999994	NS
IV muGFP--IV muGFP+	0,173472138	NS
IV muTOT-IV muGFP+	0,999386686	NS
TAmu p10-IV muGFP+	1	NS
IV muTOT-IV muGFP-	0,658911978	NS
TAmu p10-IV muGFP-	0,174422135	NS
TAmu p10-IV muTOT	0,999406787	NS

table S2. Differential expression of RNA-seq profiles of μ and TAμ cell populations. See Excel file.

table S3A. Genes up-regulated in μCT versus μBU_TX as per Fig. 5A.

table S3B. Genes down-regulated in μCT versus μBU_TX as per Fig. 5B.

table S3C. Genes up-regulated in μCT versus TAμBU_TX as per Fig. 5C.

table S3D. Genes down-regulated in μCT versus TAμBU_TX as per Fig. 5D. See Excel file.

table S4. Moderated *t* test (limma) after FDR (*46*) adjustment for the different contrast of interest.

	CONTRAST					
	µ.BUTX vs TAµ.BUTX	**µCT vs µBUTX**	**p10.TAµ vs µ.BUTX**	**µCT vs TAµ.BUTX**	**p10.TAµ vs TAµ.BUTX**	**µCT vs p10.TAµ**
Up in p9						
Scd2	0,08811	0,00055	0,54206	0,00002	0,05929	0,00002
Psat1	0,72021	0,00835	0,00103	0,02209	0,00146	0,00002
Fcrls	0,71736	0,00634	0,11386	0,02288	0,04923	0,00003
Crybb1	0,42750	0,24540	0,01303	0,04204	0,00336	0,14771
Csf1	0,33430	0,47249	0,00486	0,08511	0,00764	0,00841
Up in adult						
Selplg	0,00073	0,13772	0,00001	0,00147	0,51103	0,00027
Mafb	0,87034	0,01088	0,00001	0,00771	0,00005	3,70E-08
Mef2a	0,69680	0,69008	0,00065	0,34090	0,00778	0,00012
Pmepa1	0,00519	0,04092	0,00119	0,00004	0,00000	0,23371
Cd14	0,12897	0,41616	0,72535	0,01310	0,07105	0,11675